

1 ***When feeling is better than seeing: Adult Zebrafish Ignore Wide-Field Optic-Flow in***
2 ***Laminar, but not Turbulent Hydrodynamic Environments.***

3

4

5 Dave, S.¹ and Liao, J.C.^{2*}

6 ¹ Department of Biology, Case Western Reserve University, Cleveland, OH 44106, USA.

7 ² Department of Biology, University of Florida, The Whitney Laboratory for Marine Bioscience,
8 9505 Oceanshore Blvd, St Augustine, FL 32080, USA.

9 *Corresponding Author & Lead Contact: J.C.L (jliao@whitney.ufl.edu)

10

11 Key words: swimming, fish, schooling, station holding, escape, turbulence, optomotor
12 response, lateral line.

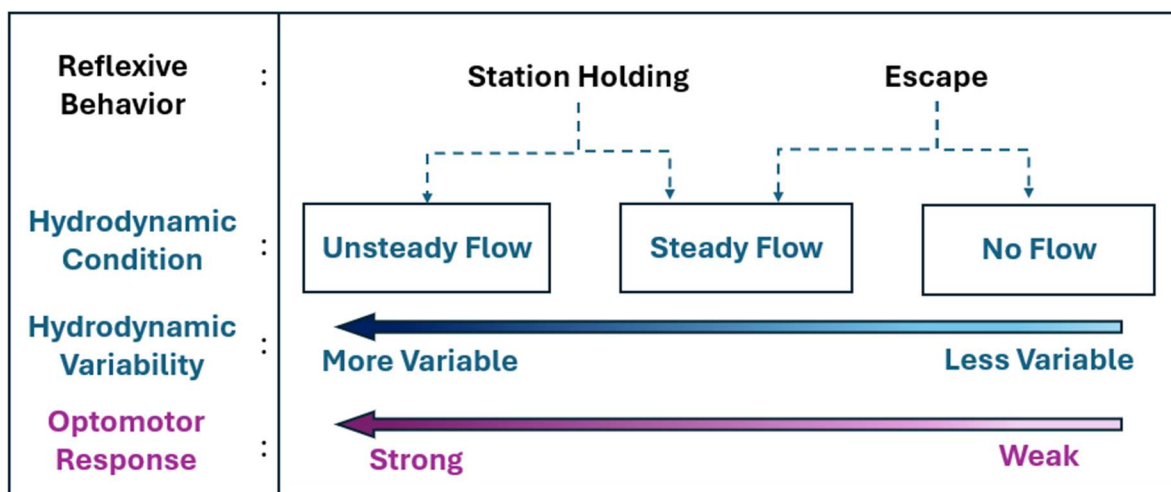
13 Abstract

14 Many animals navigate their world largely by seeing and feeling it. To disentangle these visual
15 and mechanosensory contributions, we developed a virtual reality assay targeting the
16 optomotor response in adult wild-type zebrafish swimming against flow. By projecting dynamic
17 visual patterns onto the walls of a variable-speed flow tank, we decoupled wide-field optic flow
18 from hydrodynamic velocity. We then tested fish responses to abrupt visual perturbations
19 while they held station in the unsteady wake behind a bluff body. These perturbations reliably
20 elicited compensatory optomotor responses, with fish aligning to the direction of the moving
21 stimulus. Notably, this behavior was absent in uniform flows, suggesting that fish prioritize
22 visual input when predictive lateral line signaling is compromised. We propose that this
23 sensory shift serves to optimize swimming energetics in turbulent wakes. Extending this
24 framework, we further show that zebrafish swimming against flow, whether alone or in groups,
25 exhibit heightened escape responses to looming visual stimuli. Together, our findings reveal
26 that fish sensory strategies are not fixed but dynamically tuned to hydrodynamic context:
27 favoring visual cues in turbulent environments and lateral line input in uniform flows.

28

29 Graphical Abstract

30



31 **Introduction**

32 Sensory cues from different modalities often arrive simultaneously or overlap in sequence,
33 providing animals with a rich and redundant source of information to navigate novel and
34 complex environments. A growing acknowledgment of the integration and conflict dynamics of
35 multiple sensory modalities (vision is coupled with olfaction, air flow, vestibular, etc.) has led
36 to new insights in interpreting and understanding behavioral responses at the organismal
37 level.

38 Animals moving through water experience vastly different challenges from terrestrial animals.
39 In particular, the higher density and viscosity of water, the forces currents can create, and the
40 relative lack of light characterize aquatic and marine habitats where vertebrate life originated.
41 For over 400 million years, fishes have evolved to integrate mechanosensory and visual
42 information to shape their behavior and ecology. The lateral line and visual system, detecting
43 water flow and light, play a critical role in this integration, enabling fish to navigate and
44 respond to their environment. The lateral line is an ancient mechanosensory system that
45 predates the evolution of visual systems in vertebrates, and detects predators, prey,
46 conspecifics and water currents. Specifically, genes associated with mechanosensation
47 appear earlier in evolution than those related to visual processing (Šestak et al., 2013). This
48 suggests that sensing water flow and pressure was a foundational capability for early aquatic
49 vertebrates. However, despite the growing interest in understanding how multiple sensory
50 systems orchestrate behavior (Dallmann et al., 2023; Sharma & Sponberg, 2023), our
51 understanding of mechanosensation and vision in aquatic animals remains static and poorly
52 understood.

53 In contrast to the highly stochastic nature of ambient turbulent flows, which, when interacting
54 with environmental structures (rocks, vegetation, other animals), produce vortices of widely
55 varying spatial and temporal scales, the boundary layer flow over a swimming fish's skin (and
56 thus lateral line system) is relatively predictable and repeatable (Gray, 1968). When flow
57 interacts with a simple geometric shape like a cylinder, a vortex street can be generated. Fish
58 can recapture the energy of these vortices to hold station in flow (e.g. maintain position
59 relative to the Earth frame of reference). Fish holding station behind a cylinder show

60 drastically reduced oxygen demands, saving up to half the cost of swimming compared to
61 when swimming in laminar flow (Taguchi & Liao, 2011). Due to the turbulent regime in a
62 vortex street, flow unpredictability causes destabilizing movements in these surfing fish (Liao
63 et al., 2003b; Tritico & Cotel, 2010). Consistent with this, fish with an ablated lateral line avoid
64 turbulence vortex streets and prefer to station holding in areas of smoother flow, suggesting a
65 reliance on detecting flows to maintain position while station holding (Liao, 2006). Turbulence
66 may limit the capabilities of the lateral line to signal normal swimming movements, where
67 muscle commands align with sensory expectations. Predictable flow across the body is critical
68 for the lateral line to generate an image of efficient swimming, enabling a proprioceptive
69 function (Skandalis et al., 2021).

70 How does the hydrodynamic environment influence the reliance on visual information for
71 station holding in adult zebrafish? We hypothesize that fish swimming in turbulence shift their
72 sensory reliance from the lateral line towards vision. Here, we develop a novel virtual reality
73 assay in a flow tank that decouples visual and hydrodynamic sensory inputs for freely
74 swimming fishes. We use this approach to investigate the interplay between vision and the
75 lateral line during optomotor and loom behaviors across laminar and turbulent flow conditions.
76 We address previously inaccessible questions on the effect of wide-field visual on fish
77 swimming and escape behaviors in flow. By decoupling and placing into conflict visual and
78 hydrodynamic stimuli, our approach allows investigation into multi-agent and multisensory
79 integration of fish behavior.

80

81 **Materials and Methods**

82 Animals

83 We used adult (>60 dpf) WT zebrafish, *Danio rerio* (body-length, mean \pm SE = 38.6 \pm 0.7 mm,
84 n=20 fish) raised in the UC Santa Barbara zebrafish facility and transferred to the
85 experimental room >2 weeks prior to experiments. There, fish were maintained in two 10 L
86 freshwater tanks maintained at 23 \pm 0.5 °C) with a commercial aquarium heater (Eheim Co.),
87 kept on a 12:12 light:dark cycle and fed commercial pellets *ad libitum* daily. Prior to the start

88 of an experimental trial, an individual fish was introduced into the flow tank and left for 10
89 minutes to acclimatize at a current velocity of 10 cm s^{-1} (e.g. ~ 2.5 body-lengths s^{-1}). We found
90 this flow velocity would elicit the most reliable station holding response. All experimental trials
91 were conducted in the afternoon (12:00-17:00 PST) in a room enclosed by blackout curtains.
92 After data were collected from swimming trials, fish were euthanized with an over-dose of MS-
93 222.

94 Experimental Setup

95 **Flow tank:** All experiments were conducted using a custom-built 5 L recirculating flow tank
96 with a working section of $22 \times 7 \times 7 \text{ cm}$ (length x width x depth). Water flow was generated by
97 a variable speed AC-DC series motor (Dayton model 2MO37A, 115v 1.5 Amp, Lake Forest
98 Illinois USA) driving a propeller that circulated water through 2 sets of honeycomb collimators
99 ($1/8$ " aperture diameter) to generate uniform flow. Flow velocity was set at 10 cm/s and verified
100 by tracking suspended plastic particles within the working section of the flow tank. The cross-
101 sectional area of the fish was less than 5% of the cross-sectional area of the flow tank,
102 minimizing any solid blocking effects (Bell & Terhune, 1970). Water was filtered, aerated, and
103 maintained at room temperature of $22.1 \text{ }^\circ\text{C}$ ($\text{SE}=0.1^\circ\text{C}$) throughout the experiment. (See
104 Figure-1A)

105 **Visual Projection:** We used a system of mirrors (See Figure-1B) to project visual stimuli on
106 customized rear-projection screens mounted to the flow tank walls. For wide-field grating
107 patterns on the sidewalls, we varied orientation and motion (vertical gratings moving
108 downstream/upstream; horizontal gratings moving up/down) and set the optic-flow speed as
109 *ca.* 10 cm s^{-1} (spatial frequency= $1.8 \text{ cm cycle}^{-1}$, temporal frequency as 5.5 cycle s^{-1}) to match
110 hydrodynamic flow velocity. We recorded these moving projection patterns using a high-
111 speed camera at $1000 \text{ frames s}^{-1}$ to verify optic flow rates. For visual looming stimulus, we
112 used an exponentially expanding (doubling-time: diameter= 50 ms , area= 25 ms) dark-circle with
113 a bright background presented on the top-wall. Fish were acclimatized for 5 minutes before
114 each trial with either horizontal or vertical gratings on sidewalls in case of station-holding, or
115 plain white background on the top-wall in case of escape trials. For each fish trial, the

116 treatments order was randomized to evoke a reflexive response and avoid contribution due to
117 learning and memory.

118 **Filming and Digitization:** A monochromatic Chronos 1.4-HD high-speed video camera (1024
119 x 1024, 1000 frames/s, Burnaby BC Canada) was aimed at a front-surface mirror angled at
120 45° and placed directly below the working section to film the swimming kinematics and
121 position of zebrafish (Figure-1B). An LED panel with white lights and overlaid diffuser was
122 used to optimize the image contrast of the fish. In loom experiments, this panel was replaced
123 with a projection screen for the top-projected loom stimulus with against a uniform
124 background illumination. We used a semi-supervised machine-learning based tool,
125 DeepLabCut (Mathis et al., 2018), that allowed us to reliably track 4 points on fish (head-tip,
126 tail-tip, right- and left-pectoral fin base). To create a training-set, we manually labelled these 4
127 points in a total of 800 frames, randomly picked from 40 videos, and trained a neural network
128 model for ~1 million iterations to minimize the tracking error. We subsequently used this
129 model to track points on more than 400,000 frames from 80 video recordings. Tracked videos
130 using DeepLabCut were visually verified and approved before further analysis (Mathis et al.,
131 2018).

132 Experimental Design and Data Analysis

133 We studied the effects of hydrodynamic and visual conditions on freely swimming adult
134 zebrafish using two widely studied behaviors, Station-holding and Escape behavior. Below
135 are the experiment specific details for each behavior.

136 **(i) Station-Holding Behavior:**

137 Water-flow conditions – Steady / Unsteady: Many fish routinely swim against water current to
138 navigate, a behavior known as rheotaxis. These fish may experience Steady (laminar) or
139 Unsteady (turbulent) water-flow. However, station holding fish would naturally experience
140 unsteady water-flow as they swim behind rocks or bluff bodies to get help from eddies and
141 conserve energy. We studied sensory prioritization in the position-maintaining fish in a flow
142 tank and challenged them with steady and unsteady water-flow conditions. Steady flow
143 conditions were generated by a custom 3D printed honeycomb flow-straightener. D-section

144 cylinders (0.5-1 cm diameter) were added in an upstream location in the working section to
145 create a distinct flow refuge to generate suitable unsteady flow (Liao et al 2003b).

146 Linear perturbations – Optical-Pull / Push: We first tested the role of wide field visual
147 perturbation on a station holding adult fish. As the fish is swimming against water-flow, we
148 externally provided wide-field optic-flow by suddenly moving the surroundings in (i.e.,
149 vertically oriented visual gratings) forward (upstream) or backwards (downstream) directions.
150 The fish typically experience optic-flow either during self-movements or when external factors
151 (such as water-flow) move them. Since our treatments induced the optic-flow analogous to
152 fish moved by external factors, we call them ‘optical-push’ and ‘optical-pull’, based on the
153 direction of optic-flow generated. ‘Optical-push’ is the treatment of moving visual surroundings
154 from back to front of the fish, mimicking the optic-flow direction if fish are pushed backwards
155 externally (e.g., sudden increase of water-flow speeds). Similarly, optical-pull treatment will
156 suddenly move wide-field visual patterns from front to back (i.e., in a downstream direction)
157 mimicking a scenario when a station holding fish is pulled forward due to external factors
158 (e.g., sudden decrease of water-flow speeds). The prefix “optical” here refers to the fact that
159 it’s a purely visual perturbations, rather than changing waterflow speed to move the fish.

160 Rotational perturbations – Optical-Roll: We further checked the effects of a conflicting optic-
161 flow on station holding fish, where the optic-flow presented along rotational axis whereas the
162 water-flow remained linear (along the body-axis). We moved visual surroundings (i.e.,
163 horizontally oriented visual gratings) in opposite directions on each side wall at the same
164 spatial and temporal rates as the ‘Optical-Push / Pull’ treatments (see Methods: Visual
165 Projections). We call them ‘optical roll’ treatments that would mimic optic-flow generated to
166 the fish if it is externally rotated in Roll-direction (around the longitudinal-axis). The rotational
167 optic-flow is either in clockwise (CW: right-side moving down, left moving up) or
168 counterclockwise (CCW: right-side moving up, left moving down) directions from the fish’s
169 perspective.

170 Data Analysis: To examine the effect on station holding behavior, we compared 1 second of
171 fish trajectory data before and after the stimulus and quantified changes in body position,
172 swimming velocity, and tail beat. We excluded the first 500ms of data after the stimulus onset

173 from this analysis. Swimming velocity was divided into longitudinal (along the direction of flow)
174 and lateral (side-ways) directional components to better explain the behaviors observations.
175 Changes in trajectory pattern were quantified using Spearman's rank correlation (ρ), which
176 measures monotonic changes in the position (where a constant upstream movement = 1, and
177 downstream = -1). We also tracked the distal end of tail and quantified its average cyclic
178 movement amplitude and frequency over a given duration for each trial.

179 **(ii) Escape Behavior:**

180 Experimental Treatments: We studied another naturalistic behavior that is known to involve
181 vision, an escape behavior, to further compare how fish use vision in different hydrodynamic
182 conditions. We presented an exponentially expanding (looming) stimuli (see Methods: Visual
183 Projections) at the top wall of swimming chamber while fish were challenged to swim against
184 water-flow (Flow) and when at rest (No-Flow). We studied fish's response when alone in the
185 chamber (Single) or when in a group of five individuals (Group). The looming stimulus
186 generally originated towards the upstream side of the chamber, giving better visibility to the
187 fish swimming against the flow. However, we also carried out a treatment where the position
188 is shifted towards the downstream side of the chamber (Downstream Loom), to study any
189 possible effects arising due to the stimulus position.

190 Data Analysis: We studied fish's reflexive escape responses involving sudden bending of the
191 body, known as C-Start, upon presenting the looming stimulus. From the video recordings, we
192 find fish's instantaneous position w.r.t. the stimulus origin in horizontal plane ($[px, py]$ cm) and
193 the instantaneous stimulus radius (R cm) at the time of an escape response (i.e., onset of C-
194 start reflex). Vertical position of the fish (pz cm) is considered as the flow-tank height, as the
195 fish were found swimming at the bottom of the tank. From the escaping fish's three
196 dimensional position ($P=[px, py, pz]$ cm) and stimulus radius (R), we can then calculate the
197 threshold stimulus angle (θ) from the fish's perspective that elicited the escape response
198 (using the formula: $\theta = 2 \cdot \arctan(R / \text{Norm}(P))$). We call this angle (θ) the Perceived
199 Loom Angle. We also measured the escape response delay as the time difference between
200 beginning of the looming stimulus and the C-start.

201 **Results**

202 Prioritizing vision depends on hydrodynamic environment

203 We quantified fish swimming performance and their responses to wide-field visual
204 perturbation (Optical-Pull and -Push treatments, see methods: Exp. Design) while swimming
205 against steady and unsteady water currents in the flow-tank. For each treatment, we observed
206 responses from 4 adult zebrafish and repeated 4 trials for everyone, making a total 16 unique
207 trials per treatment. We used Wilcoxon signed-rank test to compare behavior responses
208 between the pre-stimulus and post-stimulus values.

209 Fish do not rely on optic-flow to maintain swimming position in steady flows

210 During trials with steady (laminar) flow, fish's swimming velocities in the streamwise direction
211 remain unchanged after the stimulus onset when compared to the pre-stimulus adaptation
212 period for Optical-Pull (velocities mean \pm s.e.m.: pre-stim = -0.2 ± 1.2 cm/s, post-stim = $0.2 \pm$
213 1.2 cm/s; $p = 0.90$, n.s.) and, also for Optical-Push treatments (velocities mean \pm s.e.m. : pre-
214 stim = -0.1 ± 1.0 cm/s, post-stim = -0.9 ± 1.1 cm/s; $p = 0.74$, n.s.). Conversely, presenting
215 exactly the same visual stimulus but now with unsteady (turbulent) currents elicited
216 stereotypical compensatory optomotor response (Figure-2 C,D). In unsteady flow, swimming
217 velocities in streamwise-directions reduces for Optical-Pull (velocities mean \pm s.e.m.: pre-stim
218 = -0.2 ± 0.4 cm/s, post-stim = -4.2 ± 0.6 cm/s; $p = 0.0004$), whereas it increases for Optical-
219 Push treatment (velocities mean \pm s.e.m.: pre-stim = -0.3 ± 0.6 cm/s, post-stim = 2.3 ± 0.6
220 cm/s; $p = 0.009$). This behavior can be explained as positive optomotor response (OMR),
221 since the fish's post-stimulus displacement is in the same direction as the visual projections
222 on sidewalls, for both Optical-Pull and Push perturbations in unsteady water currents. A
223 compensatory positive OMR may help station-holding fish to maintain its position using visual
224 feedback. Such OMR is missing for both the treatments in steady currents, suggesting a
225 prominently non-visual sensory mechanism to maintain position.

226 Fish move monotonously with wide-field optic flow in unsteady flows

227 We compared fish's trajectories with a purely linear model trajectory (with a slope=1) and
228 quantified Spearman's correlation coefficient (ρ) to study the monotonicity of their
229 responses for each treatment. ρ values of 1 and -1 represent a perfectly monotonous
230 change of position in the forward and in backwards direction, respectively. We found that fish
231 swimming in unsteady flows showed a higher monotonous change in their body position post-
232 stimulus onset. ρ value for Optical-Pull ($\rho \pm \text{s.e.m}$: pre-stim = -0.2 ± 0.2 , post-stim = $-$
233 0.8 ± 0.1 , $p=0.009$) representing a monotonous downstream drift, and for Optical-Push ($\rho \pm$
234 s.e.m : pre-stim = -0.2 ± 0.2 , post-stim = 0.6 ± 0.1 , $p=0.04$) representing largely monotonous
235 upstream surge, post stimulus onset in unsteady flows. However, when in steady flows, the
236 ρ values are spread across the spectrum with averages close to zero representing a lack of
237 overall monotonous movements (Optical-Pull: pre-stim = 0.0 ± 0.2 , post-stim = 0.0 ± 0.2 , $p=0.99$,
238 n.s.; Optical-Push: pre-stim = 0.1 ± 0.2 , post-stim = -0.1 ± 0.2 , $p=0.74$) (Figure-2).

239 Compensatory OMR only present for streamwise (longitudinal) direction

240 For both steady and unsteady hydrodynamic conditions, the post-stimulus change in position
241 happened in the streamwise direction (Figure-2, longitudinal), in the same direction as the
242 visual stimulus. Cross stream (e.g. lateral) position, velocity, and Spearman ρ values remain
243 unchanged post-stimulus (Figure-S1, all $p>0.4$, n.s.). We further found that when presenting
244 optical-roll perturbations (i.e., clockwise and counter-clockwise), fish did not display an OMR
245 either in longitudinal or lateral directions (Figure-S2, all $p>0.4$, n.s.). We also note that fish did
246 not turn, change its swimming direction or show an escape response (e.g., C-start) to any of
247 our wide-field visual stimuli. Raw trajectories and summary statistics values of the means,
248 s.e.m and p-values are included in supplemental material (Supp. Figure-1,2, Supp.Table-S1).

249 Thus, our results of visual perturbation experiments during station holding suggest that adult
250 zebrafish use optic-flow to maintain position while swimming against unsteady water streams,
251 and the compensatory optomotor response to optic-flow depends on the direction of optic-flow
252 and hydrodynamic conditions.

253 **Fish sensitivity to visual threats alters with hydrodynamic conditions**

254 As our previous experiment showed that fish swimming against water currents did not trigger
255 escape responses (e.g. C-start) to wide-field visual perturbations, next we presented an
256 exponentially expanding, purely visual looming stimulus on the dorsal wall of the flow tank and
257 studied their behavioral responses. We quantified fish's escape attempts responses (C-start)
258 due to looming stimulus presented during swimming against water current (Flow) and no
259 currents (No-Flow), both for the individual trials (Single) or when schooling (Group) (Figure-3).
260 We used Wilcoxon rank-sum test to compare quantities between Flow and No-Flow
261 treatments.

262 Escape Distance-Delay relationship depends on hydrodynamic conditions

263 Adult zebrafish escape responses for both Single and Group trials showed that the escaping
264 fish were positioned closer to the stimulus origin as compared to the non-escaping fish. This
265 relationship between the escape response presence and the distance from stimulus are
266 consistent across hydrodynamic conditions, Flow (distance mean \pm s.e.m.: Escape = 48.5 ± 6.3
267 mm, $n=36$; No-Escape = 93.7 ± 7.2 mm, $n=53$; $p=9.1e-6$) and No-Flow (Escape = 41.8 ± 4.2
268 mm, $n=41$; No-Escape = 60.3 ± 6.4 mm, $n=48$; $p=0.002$) (Figure-3A). Thus, we considered
269 fish's position when triggering a C-start response in our subsequent analysis of the behavior.

270 We also quantified the escape response delay since the start of looming stimulus expansion
271 for each of the escaping fish in all trials and studied its relationship with fish's distance from
272 stimulus to find whether closely positioned fish escaped faster. Flow trials show a stronger
273 positive relationship (slope $m = 0.20$ for Single, $m = 0.24$ for Group) when fishing swimming
274 against current than in No-Flow trials (slope $m = 0.05$ in Single, $m = 0.04$ in Group) (Figure-3
275 B). We then performed linear regression analysis because raw slope values are susceptible to
276 any mismatch in axis ranges for distance and delay. Combining escape events from Single
277 and Group trials, we found a stronger escape distance-delay correlation for the Flow
278 treatment (Pearson coefficient = 0.67 , $n=36$, $p<0.001$) than in No-Flow conditions (Pearson
279 coefficient = 0.21 , $n=41$, n.s.). This analysis shows that the fish that were swimming against
280 flow triggered C-start sooner when located closer and later when further away from the

281 stimulus. Whereas the non-swimming fish in general did not show such response, suggesting
282 they just responded to the presence of the threatening stimulus.

283 Station holding fish show a lower threshold-angle to looming stimulus

284 The escape behavior may be better studied by quantifying the threshold stimulus angle for
285 each escaping individual because it would account for both the response delay and fish's
286 distance from the stimulus. We calculated the threshold stimulus angle of the looming
287 stimulus from the perspective of the fish in three-dimensional space at the time of escape to
288 test whether station holding fish (Flow trials) responded to the angular expansion faster than
289 in No-Flow trials, as it would be predicted by their slope-values (Figure-3B). To maintain
290 consistency across each responses, we considered all trials for which the looming stimulus
291 was originating within the lateral-visual field (153° field on right and left side each; n=50 fish)
292 for the given fish positions, and excluded data with the stimuli in their blind-spot (21° field on
293 rear side; n=5 trials) and binocular (33° field on front; n=22 trials) (Pita et al., 2015). This
294 allowed us to better compare our data across Flow and No-Flow trials because fish's body
295 orientations are not always facing upstream when not swimming, as they would while
296 swimming against water currents (No-Flow trials).

297 We found that station holding fish triggered an escape at a lower stimulus angle in Flow as
298 compared to stationary fish in No-Flow (Figure-3C). These angles are plotted on a model
299 looming stimulus to visualize their median threshold angles on the expanding visual stimulus
300 in temporal axis. Finally, combining the threshold stimulus angles from each escaping fish
301 across all the Single and Group trials, we found a lower threshold for fish swimming against
302 water current (Flow: $15.9^{\circ} \pm 3.9^{\circ}$ deg, n=21) than fish in stationary water (No-Flow: $32.6^{\circ} \pm 6.8^{\circ}$
303 deg, n=29) (Figure-3D). A lower threshold angle ($p=0.017$) to trigger a C-start reflex suggest
304 increased sensitivity to the visual threat stimuli.

305 Together, our results highlight the relationship between the optic-flow and hydrodynamic flow,
306 where fish swimming in complex water currents elevate their response to optic-flow
307 perturbations.

308

309 **Discussion**

310 The OMR is crucial for an animal's ability to maintain its position, and is particularly vital for
311 fish navigating dynamic aquatic habitats. Our research offers new insights into the adaptive
312 strategies of sensory modalities in fishes, revealing how they prioritize visual and
313 mechanosensory cues based on the predictability of their hydrodynamic environment, and
314 how these strategies influence other crucial behaviors like escape responses.

315 Developmental and Hydrodynamic Influences on OMR

316 Our study of adult zebrafish reveals a distinct OMR compared to that observed in larvae.
317 While larval zebrafish typically exhibit a positive OMR, swimming with moving bars to reduce
318 optic flow (Olive et al., 2016), adults demonstrate a negative OMR, swimming against the
319 visual motion (Bak-Coleman et al., 2015). This developmental shift likely reflects the
320 maturation and calibration of sensory and motor systems (Kohashi et al., 2012). Larvae, with
321 less developed sensory systems and limited proprioception, may primarily rely on visual cues
322 for body displacement. In contrast, fully integrated adult systems allow for the development of
323 robust expectations of flow and the accumulation of error-driven motor learning experiences
324 (Montgomery et al., 2002; Skandalis et al., 2021). This calibration enables adults to form
325 precise expectations of how lateral line (and likely vestibular) inputs correspond with visual
326 inputs in predictable hydrodynamic environments like still water or steady flow.

327 However, this calibrated expectation for sensory information, typically associated with
328 steady swimming kinematics, is violated in turbulent flows. We suggest that the positive OMR
329 observed in larvae arises because they initially rely heavily on visual inputs as they gain the
330 experience necessary to fully calibrate their mechanosensory and visual systems. A
331 compelling avenue for future investigation would be to precisely determine the developmental
332 stage at which this OMR switch occurs, and whether this transition can be accelerated or
333 delayed by specific environmental conditions like light levels or turbulence.

334 Beyond neural development, the hydrodynamic regime itself imposes distinct
335 challenges and opportunities for sensory processing. Our findings indicate that fish
336 dynamically adjust their reliance on mechanosensation versus vision in a context-dependent

337 manner, revealing a previously unrecognized prioritization strategy driven by hydrodynamic
338 predictability, which correlates with Reynolds number (Re). Larval fish operate at low
339 Reynolds numbers ($Re < 100$), where viscous forces dominate and flow patterns are highly
340 predictable. In this regime, consistent lateral line reafference from self-motion likely allows
341 larvae to prioritize visual inputs for OMR, as mechanosensory input provides a stable internal
342 reference. Conversely, adult zebrafish operate at high Reynolds numbers ($Re > 1000$),
343 routinely encountering turbulent flows characterized by complex, unpredictable vortices in
344 natural aquatic environments. When uniform flow interacts with bluff bodies, the resulting
345 vortices can significantly alter swimming kinematics (Liao et al., 2003a; Sutterlin & Waddy,
346 1975). Consequently, the lateral line system receives less predictable input than during self-
347 generated swimming in uniform flow (Crapse & Sommer, 2008). While vortices can be
348 detected (Chagnaud et al., 2007), their presence likely diminishes the lateral line's capacity to
349 provide a consistent signal for self-motion or external flow, substantially reducing its reliability
350 as an accurate indicator of effective swimming in turbulence (Skandalis et al., 2021).

351 Similar principles of context-dependent sensory reweighting have been observed in
352 terrestrial systems. For example, hawkmoths tracking moving flowers modulate their reliance
353 on vision and mechanosensation depending on ambient luminance (Sharma & Sponberg,
354 2023). In bright light, visual gain increases while mechanosensory gain decreases; in dim
355 light, the reverse occurs. This mirrors our findings in zebrafish, where lateral line input
356 becomes less reliable in turbulent flow, prompting a shift toward visual cues. In both cases,
357 animals preserve behavioral performance—flower tracking in moths, station-holding and
358 escape in fish—by flexibly reconfiguring sensory strategies. These parallels suggest that
359 adaptive sensory prioritization, rather than fixed integration, may be a widespread solution to
360 environmental uncertainty.

361 Energetic Imperatives and Adaptive Sensory Prioritization

362 The diminished reliability of lateral line input in turbulent flows, coupled with the energetic
363 imperative of station-holding, profoundly influences how fish perceive and react to their
364 environment. The drive to conserve energy strongly shapes fish behavioral choices,
365 particularly in complex flow fields, and consequently their reliance on specific sensory cues.

366 Fish exploit the energetic benefits of station-holding within vortical wakes generated
367 behind bluff bodies (Liao, 2004; Stewart et al., 2016; Taguchi & Liao, 2011). This strategy,
368 termed Karman Gaiting, involves precise positioning to reduce the energetic demands of
369 swimming (Liao et al., 2003a, 2003b). Fish actively return to these energetically favorable
370 regions after displacement, demonstrating a strong motivation to maintain such positions.
371 Optimal station-holding often occurs at a specific saddle point downstream from the obstacle,
372 where flow conditions minimize energy expenditure (Taguchi & Liao, 2011; Zdravkovich,
373 1997). Even a small displacement can lead to ejection into the higher-cost freestream, with
374 oxygen consumption twice as high (Taguchi & Liao, 2011). These substantial energetic costs
375 provide a powerful incentive for fish to actively maintain station in a specific region of the
376 wake; a benefit absent in the viscous regime occupied by larval fish.

377 This drive leads to a marked shift in sensory prioritization. In predictable, uniform
378 laminar flows, where lateral line inputs are reliable, OMR is absent or diminished. This
379 suggests lateral line prioritization due to its direct, rapid, and continuous feedback on the body
380 from the water flow that vision alone cannot replicate with equivalent fidelity or speed.
381 However, when station-holding fish encounter the unpredictable, noisy hydrodynamic cues of
382 a turbulent wake, vision rises to a paramount role. This results in the emergence of a positive
383 OMR, where fish swim in the direction of a moving visual stimulus. For a fish maintaining a
384 fixed position in a turbulent flow-field, such a visual strategy is highly adaptive. Ignoring visual
385 cues would result in costly downstream drift, or risk ejection into the high-cost freestream.
386 Interestingly, stationary near-field visual cues (e.g., the cylinder) proved insufficient to
387 maintain station-holding in turbulence, indicating that broad, wide-field visual stimuli are
388 required for this behavior.

389 Role of the Efferent System and Sensory Conflict

390 A switch to visual reliance in turbulent flows suggests an underlying neural mechanism that
391 actively modulates sensory input. We propose that the efferent system of the lateral line plays
392 a critical role in this dynamic reweighting of sensory information. The efferent system cancels
393 out flow information generated by self-movement (e.g., corollary discharge, (Crapse &
394 Sommer, 2008)), allowing zebrafish to prune afferent information correlated with swimming

395 motions and the fluid environment (Skandalis et al., 2021). This comparison of expectation
396 and sensing enables the lateral line to convey external proprioceptive abilities in simple flow
397 environments.

398 Building on this, we hypothesize that the visual system is also calibrated into this
399 proprioceptive architecture. Sensing the predictable flow across the body during anticipated
400 undulations suppresses behavioral responses stemming from wide-field visual inputs; hence,
401 fish in steady flows do not react to optical perturbations. When holding station in turbulent
402 flow, the hydrodynamic cues necessary for body positioning during swimming diminish,
403 prompting fish to switch to visual cues to guide their behavior and maintain position. In these
404 conditions, fish in our study show compensatory responses to optical push and pull
405 treatments.

406 Importantly, when station-holding fish follow downstream-drifting bars, they do not turn
407 and swim downstream, nor do they cease swimming and drift passively while still facing
408 upstream. Instead, they maintain an upstream orientation and swim slower, using a reduced
409 tailbeat frequency and amplitude. Active swimming is necessary to activate an efferent motor
410 copy, which also improves control. Swimming, through corollary discharge, could calibrate
411 flow expectations along the body, allowing fish to recognize less turbulent (e.g., more
412 predictable) flows. Such an awareness is harder to execute when swimming downstream,
413 given the antero-posterior sensitivity bias of neuromasts (Munz, 1985). Through the lateral
414 line efferent/afferent system, fish are continuously in touch with their environment. Undulating
415 the body allows fish to detect changes in turbulence, as exemplified when fish, visually
416 prompted to leave their station-holding region, eventually encounter freestream flow outside
417 the wake. This would be impossible if fish drifted downstream straight-bodied, without the
418 efferent activity to gauge body awareness.

419 Our hypothesis that the efferent system gates visual input is further supported by our
420 sensory-conflict experiments. Our optical-roll experiments reveal that visual input becomes
421 less influential when lateral line input aligns with an expected environmental model. This
422 suggests that continuous hydrodynamic input to the lateral line system overrides sudden
423 visual inputs, causing fish to disregard cross-stream moving bars when flow is moving

424 downstream (this study, (Bak-Coleman et al., 2015)). In virtual rolling scenarios, the absence
425 of dorsoventral flows typically detected by the lateral line, coupled with semicircular canal
426 inputs that do not align with the rolling movements conveyed by the visual world, further
427 highlights this sensory prioritization. This raises a crucial question: if the prioritization of the
428 lateral line over the visual system is a fundamental strategy for navigating predictable
429 environments, do these principles of context-dependent sensory weighting extend to other
430 fundamental, survival-critical behaviors? To answer this, we next investigated if this sensory
431 flexibility also applies to rapid, ecologically vital behaviors like the escape response, a well-
432 characterized behavior fish use to flee predators based on auditory, visual, or lateral line
433 stimuli (Mirjany et al., 2011).

434 Vision-Dependent Escape Responses in Flow and Group Dynamics

435 For over a century, the escape response has been a focal point of research, primarily in
436 individual fish within simplified hydrodynamic environments. While most studies have been
437 conducted in still water, fish in nature often form groups as an anti-predator response (Nadler
438 et al., 2021; Krause & Ruxton, 2002; Magurran, 1990) and frequently inhabit current-swept
439 environments. Less understood, however, is the effect of group dynamics on escape
440 behavior, where individuals must process not only visual threats but also information from
441 moving group members.

442 We observed that fish initiated escape responses more frequently when in closer
443 proximity to a loom stimulus, regardless of whether they were individuals or in a group, and
444 whether they were swimming in flow or still water (Figure-3 A, B). However, the delay in
445 response showed a stronger correlation with stimulus distance when fish were swimming in
446 flow compared to still water (Figure-3 C, D). This positive correlation between distance and
447 response delay suggests that fish are reacting to the angular expansion of the stimulus rather
448 than merely its presence. When accounting for both stimulus distance and response delay,
449 fish in flow exhibited a lower angular threshold for triggering an escape response. This finding
450 aligns with the hypothesis that fish are more sensitive to visual threats while swimming in flow
451 than in still water.

452 Our results suggest that the lateral line may be sensitized to compensate for potential
453 constraints in escape trajectories within flowing water. Unlike in still water, where escape
454 speeds and energetic costs are relatively equal in all directions, upstream escape paths in
455 flow likely result in slower bursts and higher energetic costs compared to downstream or
456 cross-stream paths (Domenici & Hale, 2019; Kohashi et al., 2012). This implies that faster
457 responses in flow are a prominent component of station-holding behavior. Indeed, faster flows
458 have been shown to elicit faster performance phenotypes in other fish species in the wild
459 (Nadler et al., 2018).

460 The heightened visual sensitivity of zebrafish in challenging hydrodynamic
461 environments demonstrates their adaptive flexibility in sensory processing. However, this
462 behavioral adaptation frequently occurs within a social context, as zebrafish intrinsically
463 associated in groups. This raises further questions about how collective dynamics influence
464 threat perception and response. We found that individuals within a group exhibited a higher
465 angular threshold for escape compared to solitary individuals. This suggests that schooling
466 favors robustness to a stimulus rather than increased sensitivity, a phenomenon also
467 documented in wild fish (Fahimipour et al., 2023). Interestingly, while schooling exposes
468 individuals to unpredictable hydrodynamic stimuli generated by conspecifics, this appears to
469 have a desensitizing effect on vision, a stark contrast to the OMR where individuals become
470 more sensitive to visual threats.

471 Rethinking the Lateral Line: Beyond Simple Flow Sensing

472 To more precisely dissect the independent contributions of the lateral line and vestibular
473 systems to sensing turbulent flow, future experiments should aim to create hydrodynamic
474 conditions that generate unpredictable flow across the body while ensuring that vortex
475 strength and size do not displace the body. This approach would allow for the investigation of
476 unreliable lateral line information concurrent with predictable vestibular input, a distinction not
477 achievable in the present study due to the absence of lateral line ablation experiments.

478 Traditional antibiotic or genetic ablations of the lateral line, by primarily targeting hair
479 cells, selectively remove afferent (incoming) flow information while leaving the efferent system

480 intact. This suggests that such ablations do not isolate the study of flow sensing alone but
481 instead introduce a more complex scenario that likely involves the unmasking of other
482 sensory modalities, such as body sensing, which complicate behavioral interpretations.
483 Building on this, we predict that fish with a non-functional lateral line, when exposed to
484 uniform flows, will exhibit behaviors analogous to those observed in turbulent flow conditions.
485 In these situations, alterations in the visual wide-field may elicit behavioral responses that
486 would typically be disregarded in a uniform flow environment (e.g., antibiotic studies, (Liao,
487 2006)). This intricate interplay among sensory modalities may represent a fundamental
488 behavioral mechanism that prioritizes robust, rapid signals from the lateral line system, and
489 may have been necessary for animals before advanced visual systems were establish
490 (Šestak et al., 2013).

491 Conclusion

492 In summary, we demonstrate that wide-field visual inputs do not alter the behavior of adult
493 zebrafish swimming in uniform flows. We argue that during uniform flow conditions, where
494 hydrodynamic stimuli can be anticipated and compared to an internal model of movement,
495 fish prioritize flow inputs from the lateral line system and/or the vestibular system over wide-
496 field visual stimuli. In contrast, fish holding station in turbulent flows alter their behavior in
497 response to wide-field visual inputs. We reason that the lateral line can no longer reliably
498 predict flow along the body in unsteady flows as it can during uniform swimming. Because
499 these fish may be less certain of their swimming state based on lateral line
500 mechanoreception, vision emerges to play a larger role in directing behavioral responses. The
501 greater energetic consequence of forfeiting position when station-holding behind a bluff body
502 makes it particularly significant that visual inputs are acted upon once lateral line inputs
503 become less predictable. Furthermore, while schooling, fish experience unpredictable
504 hydrodynamic stimuli created by other individuals, yet they exhibit a decreased sensitivity to
505 looming stimuli. Our work supports the idea that the prioritization of sensory modalities, rather
506 than simple integration, is specific to flow environments. The ability to dynamically prioritize
507 sensory inputs underscores the adaptive capacity of fish in complex and challenging
508 environments. These findings emerge from an approach that embraces more complex and

509 naturalistic experiments, and have important implications for fields ranging from neuroscience,
510 collective behavior, and robotic control.

511

512

513 **Contributions**

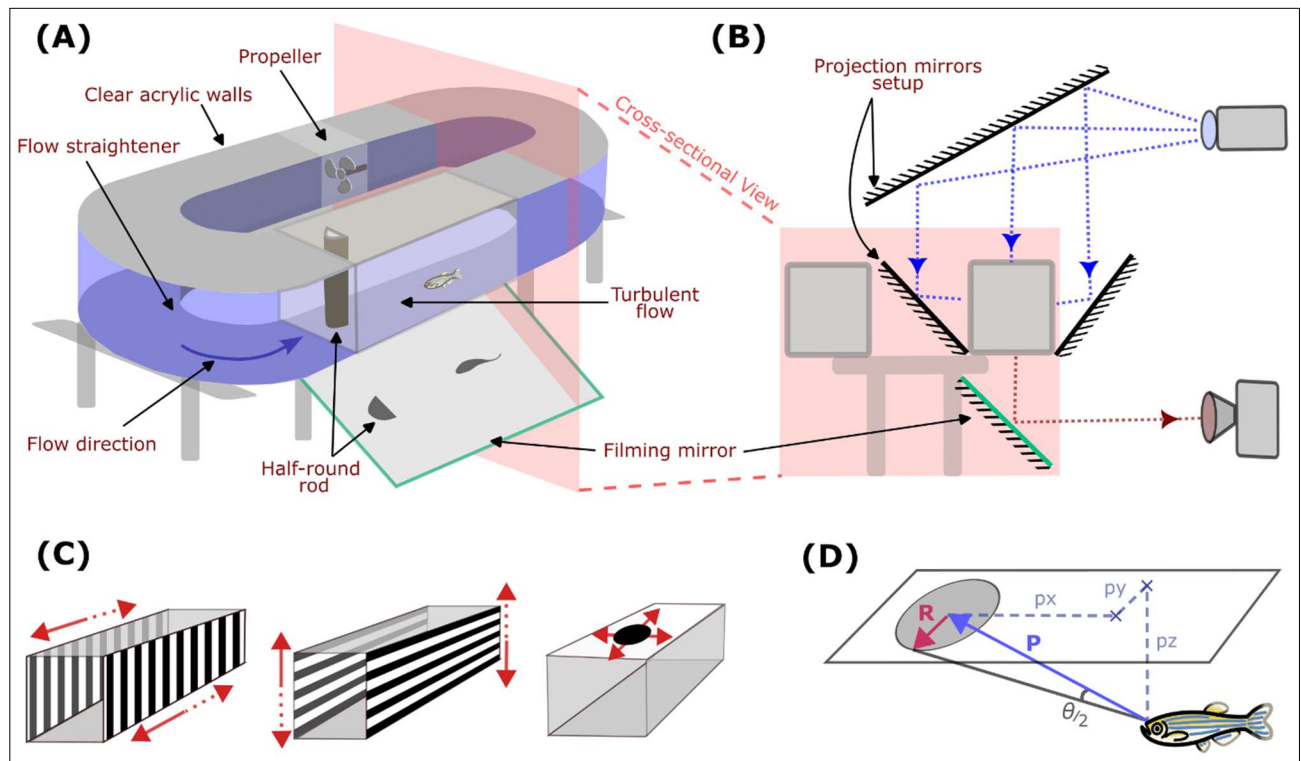
514 Conceptualization: J.C.L., S.D. Methodology: J.C.L., S.D.; Software: S.D. Validation: J.C.L.,
515 S.D.; Formal analysis: S.D.; Investigation: J.C.L., S.D.; Resources: J.C.L; Data curation:
516 J.C.L., S.D.; Writing - original draft: J.C.L., S.D.; Writing - review & editing: J.C.L., S.D.;
517 Supervision: J.C.L.; Project administration: J.C.L; Funding acquisition: J.C.L.

518

519 **Acknowledgements**

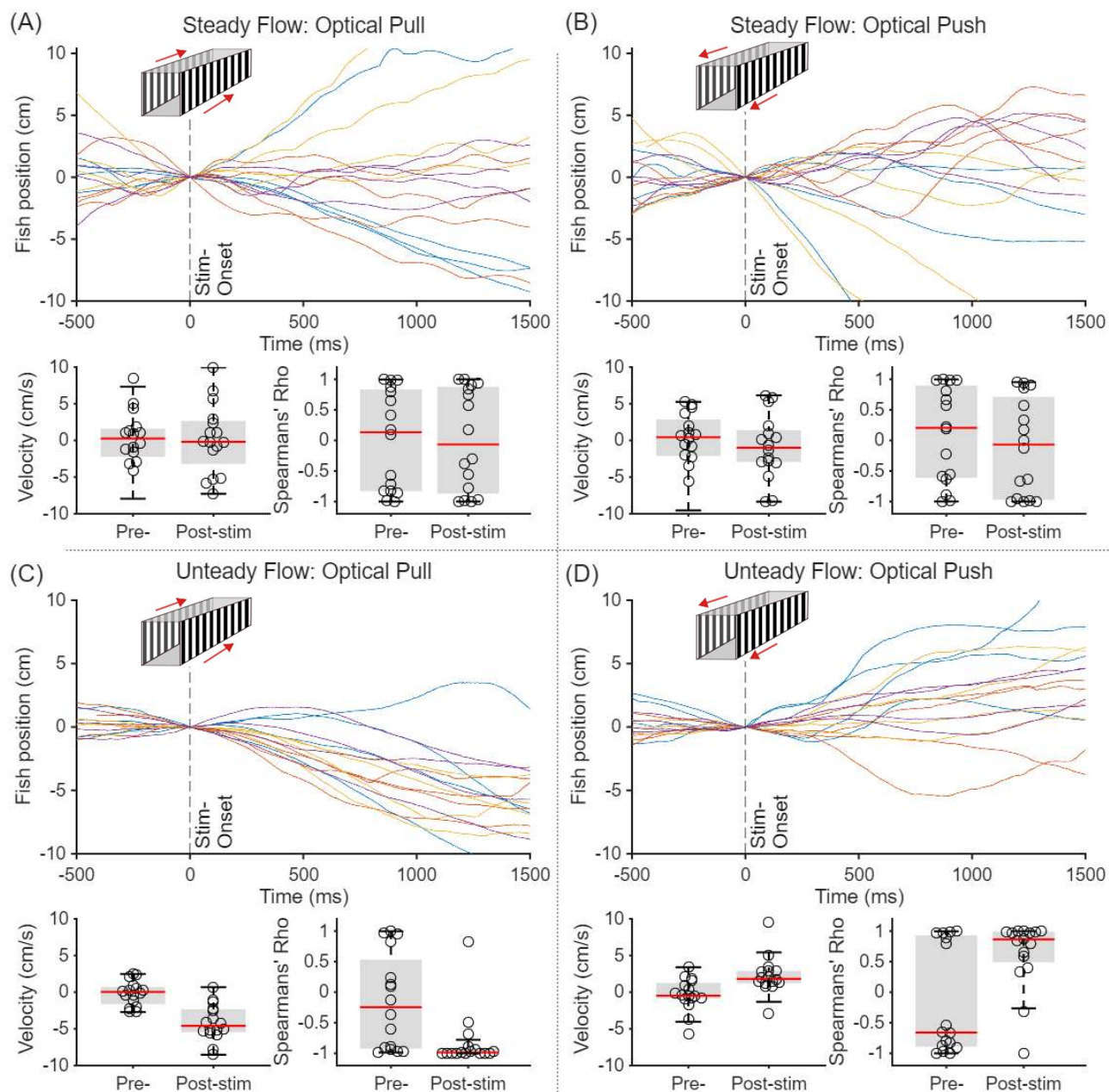
520 We would like to thank Matteo Adorisio for help with experiments and preliminary analysis,
521 and Eileen Hamilton for fish care. All protocols were approved by the University of Santa
522 Barbara Institutional Animal Care and Use Committee. This research was supported in part by
523 NSF Grant No. PHY-1748958, NIH Grant No. R25GM067110, Gordon and Betty Moore
524 Foundation Grant No. 2919.01, and the Kavli Foundation. This research was additionally
525 supported by the National Science Foundation Grants IOS 1257150, 2321275, and 1856237;
526 NSF MPS/PHY 2102891 and NSF ENG/CMMI 2345913 to J. Liao, and National Institute on
527 Deafness and Other Communication Disorders Grant R56DC020321 to J. Liao. The authors
528 declare no competing interests.

529 **Figures**



530
531 **Figure 1** – Schematic of experimental setup with the fish swimming flow-tank and visual
532 stimulus projection. (A) A variable-speed flow tank placed on a stand with a filming-mirror
533 placed underneath tilted at 45° angle to film the ventral view of the swimming fish. (B) Cross-
534 sectional view of flow tank with two side-mirrors and a top-mirror used for visual stimulus
535 projection, and filming mirror schematic. (C) Schematic of optical stimuli and their motion
536 direction, where the patterns move simultaneously in the direction of solid arrows, and then for
537 a separate treatment, move simultaneously in dashed-arrows directions. Vertical gratings for
538 “optical push/pull” and horizontal gratings for “optical roll” treatments and the expanding loom
539 stimulus on the top wall for escape trials. (D) Perceived threshold stimulus angle (θ) is
540 calculated based on the 3D position of the escaping fish and the instantaneous radius of the
541 loom stimulus.

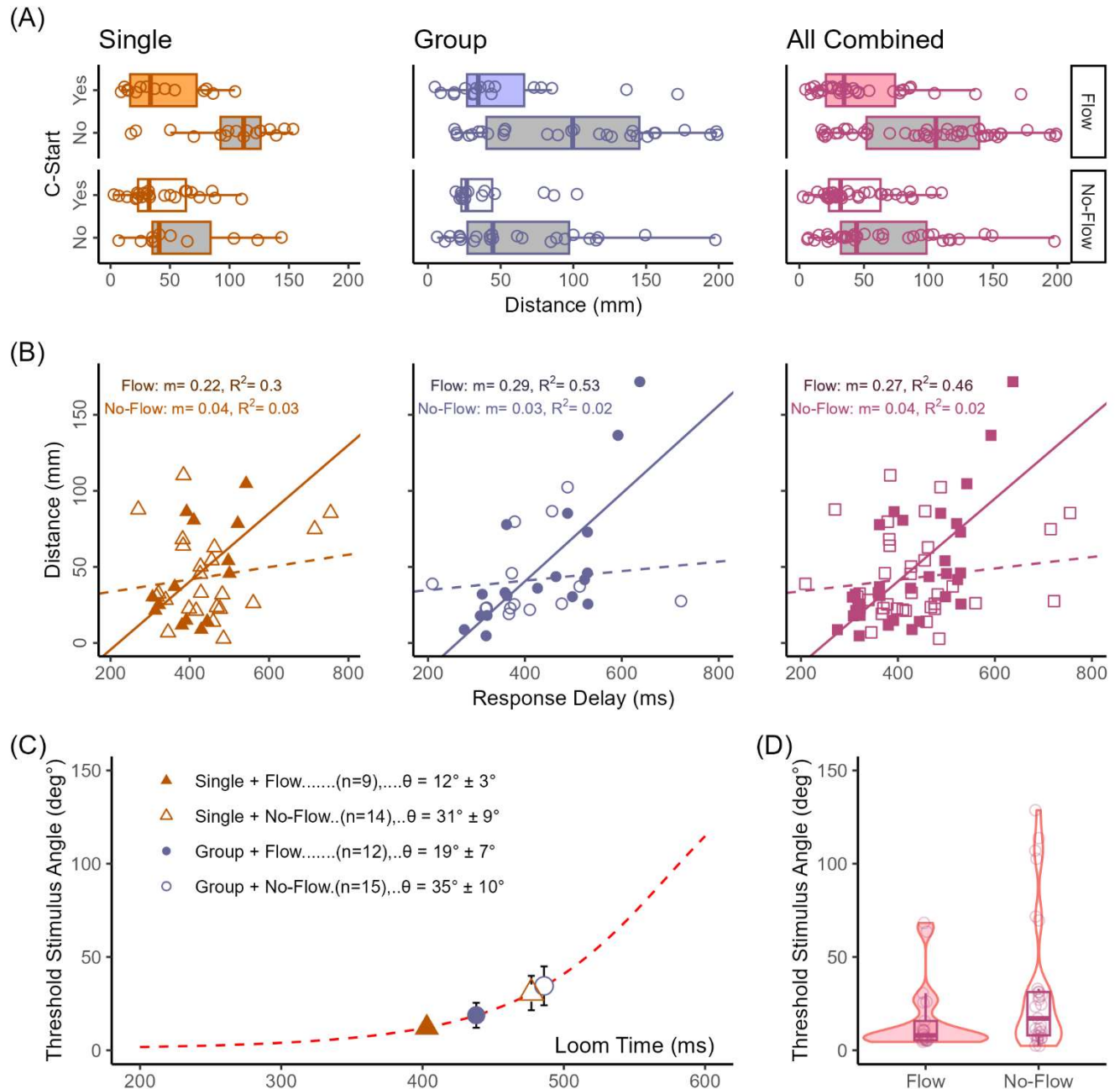
542



543

544 **Figure 2** – Quantifying station-holding fish' response to wide-field optical perturbations in
545 steady water-flow (A-B) and unsteady flow (C-D). (A,C) “Optical pull” stimulus entails visual
546 patterns suddenly moving downstream at the stimulus-onset (vertical dashed-line). *Top-panel:*
547 Fish's longitudinal positions (along the streamwise direction) is plotted against time, where
548 negative position values show downstream drift for “optical pull” (visual patterns moving
549 downstream) and each color represents one individual fish (n=4 fish, 4 trials each); *Bottom-*
550 *panel:* Comparing the change in fish's swimming velocity and Spearman's correlation co-

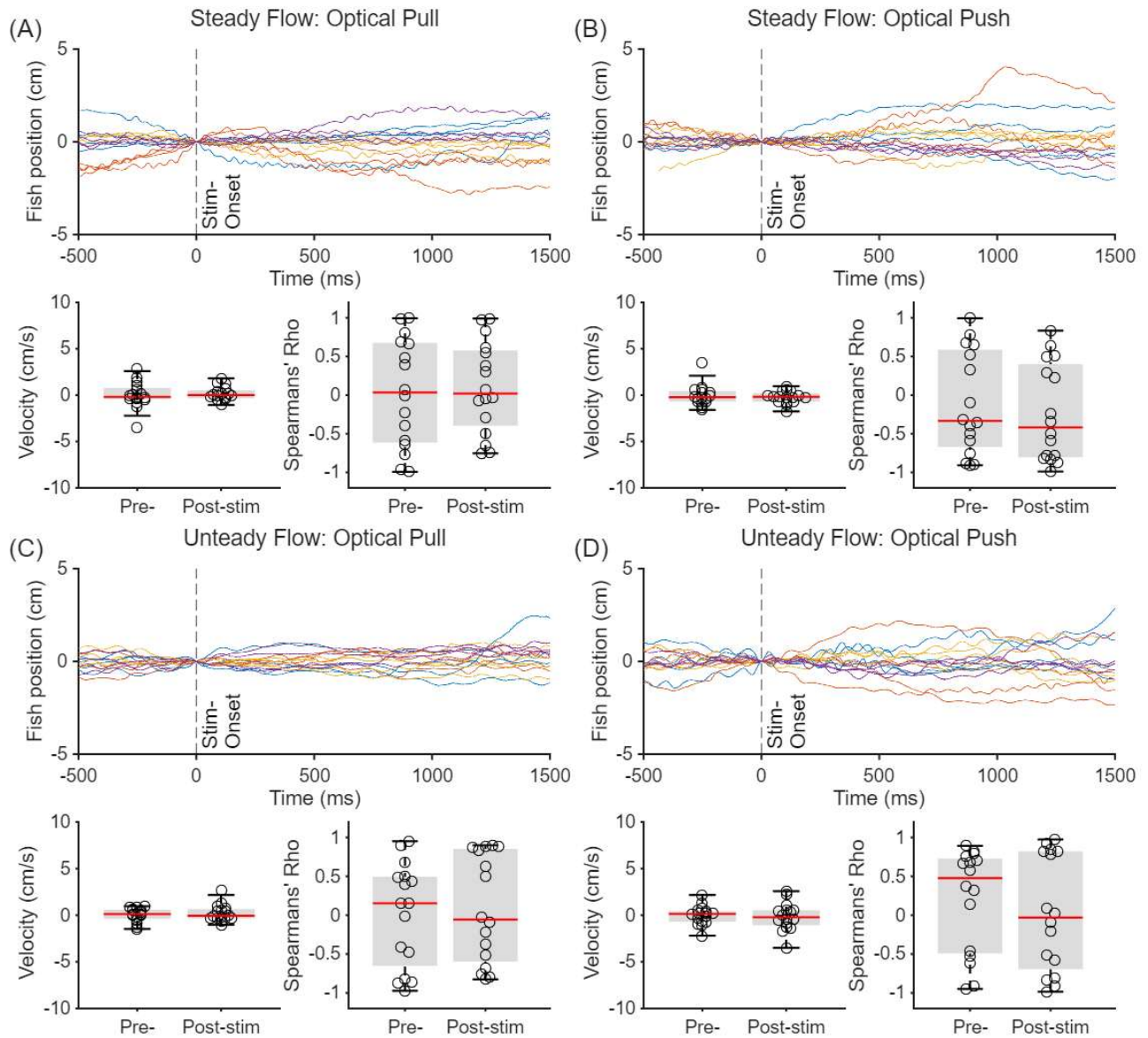
551 efficient (representing degree of monotonous movements) before and after the stimulus
552 onset. (B,D) Same plots as in part-A but for the “optical push” stimulus, where visual patterns
553 move upstream at the onset (n=4 fish, 4 trials each).



554
 555 **Figure 3** – Comparison of escape response (C-start) due to a purely visual looming stimulus
 556 during “flow” (swimming against water current) and “no-flow” (still water) conditions in
 557 individual (“Single”) and school (“Group”) of fish. (A) Presence or absence of escape trigger
 558 (C-start) is classified for “flow” (top) and “no-flow” (bottom) conditions, and plotted against
 559 fish’s swimming distance from the stimulus center point. (B) Similar to part-A but now
 560 projecting the looming stimulus on a different part (i.e., towards the downstream end of the
 561 flow-tank). (C-D) For the escaping fish, their swimming distance and response delay are

562 compared between “flow” and “no-flow” conditions. A higher slope indicates stronger
563 correlation between those quantities. (E) Perceived angle of the threshold stimuli (θ), which is
564 found using fish’s 3D position and instantaneous radius of looming stimulus, for all trials are
565 plotted on a representative looming stimulus (Dashed line) that indicates the angular
566 expansion of the looming stimulus over time. (F) The same threshold stimulus angles for all
567 the fish are compared between “flow” and “no-flow” trials. A lower angle represents quicker
568 escape.

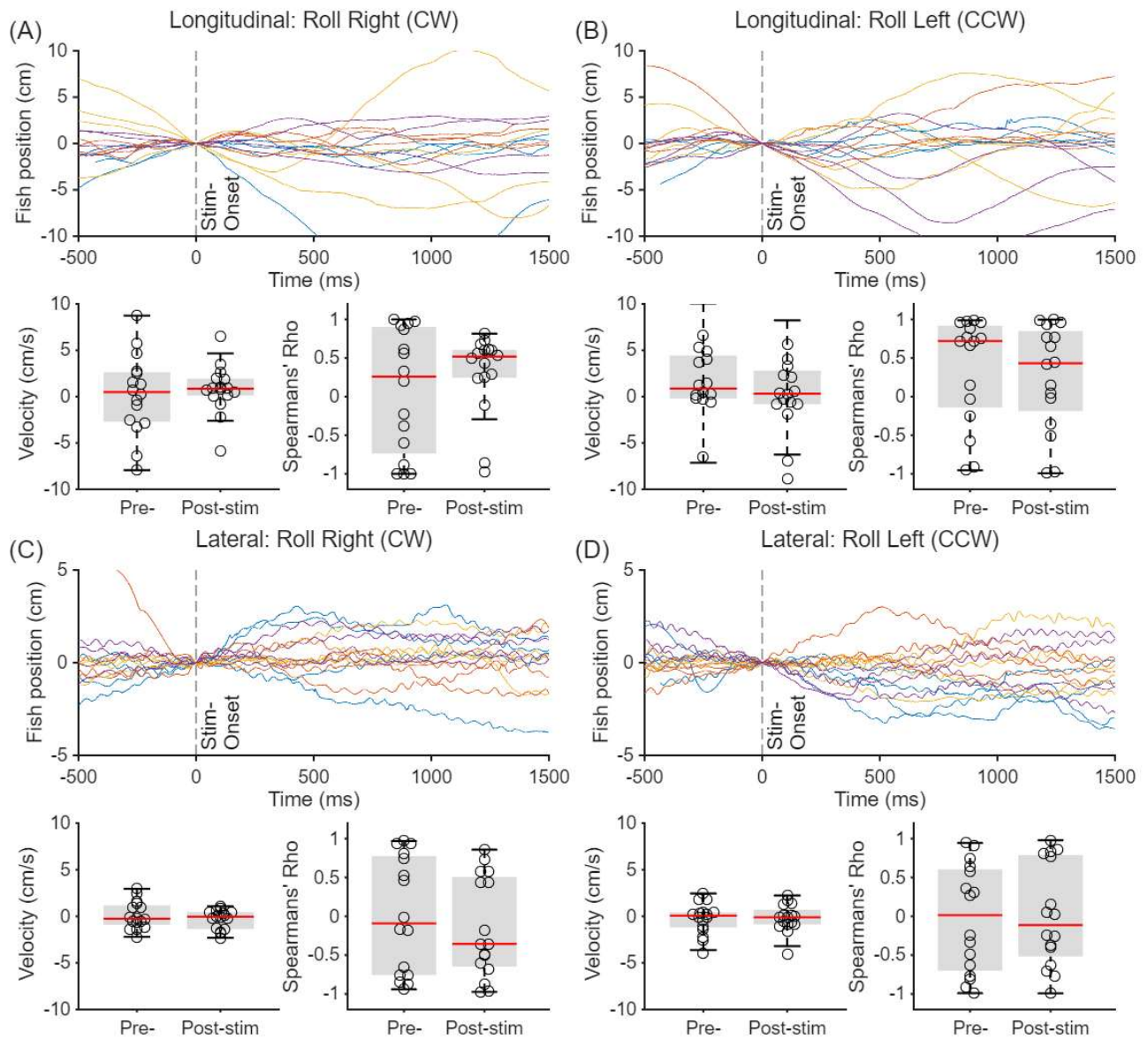
569 **Supplementary Materials**



570
571 **Supp. Figure 1** – Raw trajectory data and velocity data for lateral movements in optical
572 pull/push experiments for steady and unsteady flow (raw data for longitudinal movements,
573 and plot legends are as in Fig-2).

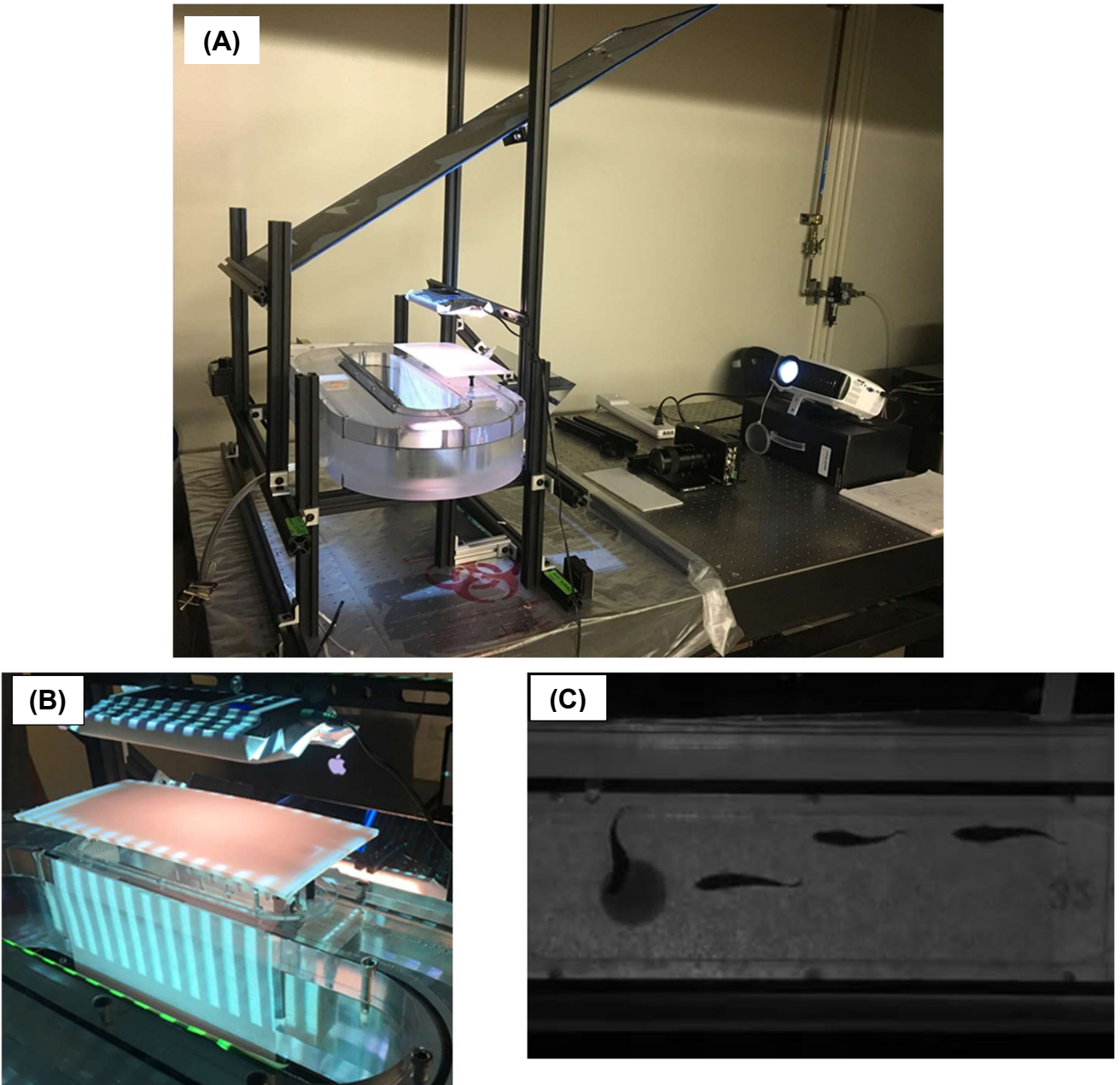
574

575



576

577 **Supp. Figure 2** – Raw data for optical roll perturbations (CW & CCW directions) for
578 longitudinal and lateral direction movements. Plot legends are similar to explained in Fig-2 (A-
579 B))



580 **Supp. Figure 3** – Images of the experiment setup. (A) Flow tank, Projection and Recording
581 setup. (B) Example visual stimulus projected on a side-wall of swimming chamber. (C) A
582 section of an image acquired by the camera of a group of fish swimming with an expanding
583 looming stimulus in the background and the first fish (from upstream side) triggering a C-start
584 reflex.

585 **Table S1 : Statistical summary of lateral-only motion in response to visual perturbation**

Lateral-Only	Side Velocity mean \pm s.e.m (cm/s)		P-val	Side rho mean \pm s.e.m		P-val
	Pre-Stimulus	Post-Stimulus	Pre vs Post	Pre-Stimulus	Post-Stimulus	Pre vs Post
Optical-Pull (Steady)	4.2E-04 \pm 3.5E-03	1.5E-03 \pm 2.0E-03	0.98 (n.s.)	3.2E-02 \pm 1.8E-01	1.0E-01 \pm 1.5E-01	0.82 (n.s.)
Optical-Push (Steady)	-3.7E-04 \pm 2.9E-03	-2.2E-03 \pm 1.7E-03	0.63 (n.s.)	-1.1E-01 \pm 1.7E-01	-2.3E-01 \pm 1.6E-01	0.60 (n.s.)
Optical-Pull (Unsteady)	3.6E-04 \pm 1.8E-03	2.3E-03 \pm 2.3E-03	0.67 (n.s.)	1.5E-02 \pm 1.7E-01	8.0E-02 \pm 1.7E-01	0.86 (n.s.)
Optical-Push (Unsteady)	-1.6E-04 \pm 2.5E-03	-1.6E-03 \pm 3.8E-03	0.74 (n.s.)	2.0E-01 \pm 1.7E-01	2.1E-02 \pm 1.9E-01	0.46 (n.s.)
Optical-Roll (cw)	-2.5E-03 \pm 4.2E-03	-1.8E-03 \pm 3.7E-03	0.98 (n.s.)	-2.6E-02 \pm 1.7E-01	6.0E-03 \pm 1.7E-01	0.90 (n.s.)
Optical-Roll (ccw)	1.2E-03 \pm 3.6E-03	-3.3E-03 \pm 2.6E-03	0.74 (n.s.)	1.4E-02 \pm 1.9E-01	-1.5E-01 \pm 1.6E-01	0.86 (n.s.)

586

587 **References**

- 588 Bak-Coleman, J., Smith, D., & Coombs, S. (2015). Going with, then against the flow:
589 Evidence against the optomotor hypothesis of fish rheotaxis. *Animal Behaviour*, *107*,
590 7–17. <https://doi.org/10.1016/j.anbehav.2015.06.007>
- 591 Chagnaud, B. P., Bleckmann, H., & Hofmann, M. H. (2007). Kármán vortex street detection by
592 the lateral line. *Journal of Comparative Physiology. A, Neuroethology, Sensory, Neural,*
593 *and Behavioral Physiology*, *193*(7), 753–763. [https://doi.org/10.1007/s00359-007-](https://doi.org/10.1007/s00359-007-0230-1)
594 0230-1
- 595 Crapse, T. B., & Sommer, M. A. (2008). Corollary discharge across the animal kingdom.
596 *Nature Reviews. Neuroscience*, *9*(8), 587–600. <https://doi.org/10.1038/nrn2457>
- 597 Dallmann, C. J., Dickerson, B. H., Simpson, J. H., Wyart, C., & Jayaram, K. (2023).
598 Mechanosensory Control of Locomotion in Animals and Robots: Moving Forward.
599 *Integrative And Comparative Biology*, *63*(2), 450–463.
600 <https://doi.org/10.1093/icb/icad057>
- 601 Domenici, P., & Hale, M. E. (2019). Escape responses of fish: A review of the diversity in
602 motor control, kinematics and behaviour. *Journal of Experimental Biology*, *222*(18),
603 jeb166009. <https://doi.org/10.1242/jeb.166009>
- 604 Fahimipour, A. K., Gil, M. A., Celis, M. R., Hein, G. F., Martin, B. T., & Hein, A. M. (2023). Wild
605 animals suppress the spread of socially transmitted misinformation. *Proceedings of the*
606 *National Academy of Sciences*, *120*(14), e2215428120.
607 <https://doi.org/10.1073/pnas.2215428120>
- 608 Gray, J. (1968). Animal locomotion [by] James Gray. In *Animal locomotion*. Weidenfeld &
609 Nicolson.

- 610 Kohashi, T., Nakata, N., & Oda, Y. (2012). Effective Sensory Modality Activating an Escape
611 Triggering Neuron Switches during Early Development in Zebrafish. *The Journal of*
612 *Neuroscience*, 32(17), 5810–5820. <https://doi.org/10.1523/JNEUROSCI.6169-11.2012>
- 613 Krause, J., & Ruxton, G. D. (2002). *Living in Groups*. Oxford University PressOxford.
614 <https://doi.org/10.1093/oso/9780198508175.001.0001>
- 615 Liao, J. C. (2004). Neuromuscular control of trout swimming in a vortex street: Implications for
616 energy economy during the Karman gait. *The Journal of Experimental Biology*, 207(Pt
617 20), 3495–3506. <https://doi.org/10.1242/jeb.01125>
- 618 Liao, J. C. (2006). The role of the lateral line and vision on body kinematics and hydrodynamic
619 preference of rainbow trout in turbulent flow. *Journal of Experimental Biology*, 209(20),
620 4077–4090. <https://doi.org/10.1242/jeb.02487>
- 621 Liao, J. C., Beal, D. N., Lauder, G. V., & Triantafyllou, M. S. (2003a). Fish Exploiting Vortices
622 Decrease Muscle Activity. *Science*, 302(5650), 1566–1569.
623 <https://doi.org/10.1126/science.1088295>
- 624 Liao, J. C., Beal, D. N., Lauder, G. V., & Triantafyllou, M. S. (2003b). The Kármán gait: Novel
625 body kinematics of rainbow trout swimming in a vortex street. *Journal of Experimental*
626 *Biology*, 206(6), 1059–1073. <https://doi.org/10.1242/jeb.00209>
- 627 Magurran, A. E. (1990). The adaptive significance of schooling as an anti-predator defence in
628 fish. *Annales Zoologici Fennici*, 27(2), 51–66.
- 629 Mathis, A., Mamidanna, P., Cury, K. M., Abe, T., Murthy, V. N., Mathis, M. W., & Bethge, M.
630 (2018). DeepLabCut: Markerless pose estimation of user-defined body parts with deep

- 631 learning. *Nature Neuroscience*, 21(9), Article 9. [https://doi.org/10.1038/s41593-018-](https://doi.org/10.1038/s41593-018-0209-y)
632 0209-y
- 633 Mirjany, M., Preuss, T., & Faber, D. S. (2011). Role of the lateral line mechanosensory
634 system in directionality of goldfish auditory evoked escape response. *Journal of*
635 *Experimental Biology*, 214(20), 3358–3367. <https://doi.org/10.1242/jeb.052894>
- 636 Montgomery, J., Carton, G., & Bodznick, D. (2002). Error-Driven Motor Learning in Fish. *The*
637 *Biological Bulletin*, 203(2), 238–239. <https://doi.org/10.2307/1543417>
- 638 Munz, H. (1985). Single unit activity in the peripheral lateral line system of the cichlid
639 fish *Sarotherodon niloticus* L. *Journal of Comparative Physiology A*, 157(5), 555–568.
640 <https://doi.org/10.1007/BF01351350>
- 641 Nadler, L. E., Killen, S. S., Domenici, P., & McCormick, M. I. (2018). Role of water flow regime
642 in the swimming behaviour and escape performance of a schooling fish. *Biology Open*,
643 bio.031997. <https://doi.org/10.1242/bio.031997>
- 644 Nadler, L. E., McCormick, M. I., Johansen, J. L., & Domenici, P. (2021). Social familiarity
645 improves fast-start escape performance in schooling fish. *Communications Biology*,
646 4(1), 897. <https://doi.org/10.1038/s42003-021-02407-4>
- 647 Olive, R., Wolf, S., Dubreuil, A., Bormuth, V., Debrégeas, G., & Candelier, R. (2016).
648 Rheotaxis of Larval Zebrafish: Behavioral Study of a Multi-Sensory Process. *Frontiers*
649 *in Systems Neuroscience*, 10. <https://doi.org/10.3389/fnsys.2016.00014>
- 650 Pita, D., Moore, B. A., Tyrrell, L. P., & Fernández-Juricic, E. (2015). Vision in two cyprinid fish:
651 Implications for collective behavior. *PeerJ*, 3, e1113. <https://doi.org/10.7717/peerj.1113>

- 652 Šestak, M. S., Božičević, V., Bakarić, R., Dunjko, V., & Domazet-Lošo, T. (2013).
653 Phylostratigraphic profiles reveal a deep evolutionary history of the vertebrate head
654 sensory systems. *Frontiers in Zoology*, 10(1), 18. [https://doi.org/10.1186/1742-9994-](https://doi.org/10.1186/1742-9994-10-18)
655 10-18
- 656 Sharma, V. P., & Sponberg, S. (2023). *Context dependent multisensory integration:*
657 *Mechanosensation depends on luminance for robust performance.* Neuroscience.
658 <https://doi.org/10.1101/2023.09.29.560224>
- 659 Skandalis, D. A., Lunsford, E. T., & Liao, J. C. (2021). Corollary discharge enables
660 proprioception from lateral line sensory feedback. *PLOS Biology*, 19(10), e3001420.
661 <https://doi.org/10.1371/journal.pbio.3001420>
- 662 Stewart, W. J., Tian, F.-B., Akanyeti, O., Walker, C. J., & Liao, J. C. (2016). Refuging rainbow
663 trout selectively exploit flows behind tandem cylinders. *The Journal of Experimental*
664 *Biology*, 219(Pt 14), 2182–2191. <https://doi.org/10.1242/jeb.140475>
- 665 Sutterlin, A. M., & Waddy, S. (1975). Possible Role of the Posterior Lateral Line in Obstacle
666 Entrainment by Brook Trout (*Salvelinus fontinalis*). *Journal of the Fisheries Research*
667 *Board of Canada*, 32(12), 2441–2446. <https://doi.org/10.1139/f75-281>
- 668 Taguchi, M., & Liao, J. C. (2011). Rainbow trout consume less oxygen in turbulence: The
669 energetics of swimming behaviors at different speeds. *Journal of Experimental Biology*,
670 214(9), 1428–1436. <https://doi.org/10.1242/jeb.052027>
- 671 Tritico, H. M., & Cotel, A. J. (2010). The effects of turbulent eddies on the stability and critical
672 swimming speed of creek chub (*Semotilus atromaculatus*). *Journal of Experimental*
673 *Biology*, 213(13), 2284–2293. <https://doi.org/10.1242/jeb.041806>

674 Zdravkovich, M. M. (1997). *Flow Around Circular Cylinders: A Comprehensive Guide Through*
675 *Flow Phenomena, Experiments, Applications, Mathematical Models, and Computer*
676 *Simulations*. Oxford University PressOxford.
677 <https://doi.org/10.1093/oso/9780198563969.001.0001>
678